Bioactive Materials 6 (2021) 1653–1662

Contents lists available at ScienceDirect

Bioactive Materials

journal homepage: www.sciencedirect.com/journal/bioactive-materials

Bio-inspired intestinal scavenger from microfluidic electrospray for detoxifying lipopolysaccharide

Cheng Zhao [a,b,c], Guopu Chen [a], Huan Wang [a,b,c], Yuanjin Zhao [a,b,c,*], Renjie Chai [a,b,d,e,f,**]

[a] Department of Rheumatology and Immunology, Institute of Translational Medicine, The Affiliated Drum Tower Hospital of Nanjing University Medical School, Nanjing, 210002, China
[b] State Key Laboratory of Bioelectronics, School of Life Sciences and Technology, Jiangsu Province High-Tech Key Laboratory for Bio-Medical Research, Southeast University, Nanjing, 210096, China
[c] Department of Endocrinology, Shenzhen Second People's Hospital, Center for Diabetes, Obesity and Metabolic Diseases of Shenzhen University, Health Science Center of Shenzhen University, Shenzhen, 518035, PR China
[d] Co-Innovation Center of Neuroregeneration, Nantong University, Nantong, 226001, China
[e] Institute for Stem Cell and Regeneration, Chinese Academy of Science, Beijing, China
[f] Beijing Key Laboratory of Neural Regeneration and Repair, Capital Medical University, Beijing, 100069, China

ARTICLE INFO

Keywords:
Biomimetic
Intestinal barrier
Microfluidics
Microcapsule
Gastrointestinal disease

ABSTRACT

Lipopolysaccharide (LPS) plays an important role in metabolic syndrome (MetS) and other gut-derived diseases, and detoxifying LPS is considered to be a fundamental approach to prevent and treat these diseases. Here, inspired by the feeding behaviour of scavenger, novel microfluidic microcapsules with alkaline phosphatase (ALP) encapsulation and the scavenger-like molecular sieve shell are presented for cleaning intestinal LPS. Benefiting from the precisely controlled of the pore size and microfluidic electrospray, the generated microcapsules were imparted with porous molecular-sieve shells and ALP encapsulated active cores. These microcapsules could continuously work as an intestinal scavenger after colonized in intestine. It has been demonstrated that the microcapsules could englobe LPS while inhibit the permeation of digestive enzyme, and this ability contributes to promising ALP's activity, protecting cells at the presence of LPS and reducing inflammation. In addition, this scavenger inspired microcapsule could effectively decrease the LPS in organs, reduce inflammation and regulating fat metabolism *in vivo*. These features make the ALP encapsulated microcapsules an ideal candidate for treating MetS and other LPS related diseases.

1. Introduction

Metabolic syndrome (MetS) is a complex syndrome associated with obesity, type 2 diabetes, hypertension, atherosclerosis and non-alcoholic fatty liver disease, reaching epidemic proportions worldwide with great burden on medicine and economic [1–3]. Recently, lipopolysaccharide (LPS) has been regarded as central to the pathogenesis of MetS [4–6]. Along with the irregular diet and routines in modern life, especially the high fat and high sugar (HFHS) diet, the morbidity and severity of MetS increases with higher intake of LPS [7–9]. So far, several approaches including chemical drugs, hemofiltration and biomacromolecules have been applied to clean LPS and cure the diseases [10–12]. Among these methods, biomacromolecules, such as intestinal alkaline phosphatase (ALP), are the most attractive candidates due to their ability in detoxifying LPS through dephosphorylation [13]. However, the direct injection or orally supplement of ALP protein leads to the short residence in body and causes loss of efficient actives [14]. This together with the intricate digestive systems and complex metabolism environment have limited the efficiency and clinical applications of ALP [15,16]. Thus, novel stratagem to utilize enzymes, which can continuously work in intestine, is still anticipated.

In this paper, inspired by the feeding behaviour of scavenger, we present a novel microfluidic microcapsule with the scavenger-like molecular sieve and the ability to clean intestinal LPS, as shown in Fig. 1. In

* Corresponding author. Department of Rheumatology and Immunology, Institute of Translational Medicine, The Affiliated Drum Tower Hospital of Nanjing University Medical School, Nanjing, 210002, China.
** Corresponding author. Department of Rheumatology and Immunology, Institute of Translational Medicine, The Affiliated Drum Tower Hospital of Nanjing University Medical School, Nanjing, 210002, China.
E-mail addresses: yjzhao@seu.edu.cn (Y. Zhao), renjiec@seu.edu.cn (R. Chai).

https://doi.org/10.1016/j.bioactmat.2020.11.017
Received 16 September 2020; Received in revised form 28 October 2020; Accepted 12 November 2020

nature, the scavenger could extract their food by filtration and purify environment through predation, which could be imitated with designing functional microcapsules. Generally, the microcapsules that with core-shell structures hold immense promise for encapsulating actives in different areas [17–21]. Thus, a number of techniques have been explored for their fabrications [22–28]. Among these methods, microfluidic techniques are most attractive as proved to overcome inherent challenges to varieties associated with the production [29–33]. However, these methods usually require organic solvents as oil phase which may denature proteins and impede their function [34–40]. In addition, due to lacking design of shell, most of the microcapsules could hardly manage a balance between a good encapsulation and well permeability, which build the barrier between bioactive contents and targets. Therefore, few researches are currently engaged in enzyme-based microcapsules for intestinal detoxification with microfluidic techniques.

Here, we employed electrostatically driven microfluidics to encapsulate the enzyme and fabricate programmable partially-degrading microcapsules with the desired features for regulating intestinal homeostasis and preventing LPS-derived diseases. It was demonstrated that the electrostatically driven microfluidics could encapsulate the contents into a core-shell structure through quick ionic crosslinking of alginate and photocuring of poly (ethylene glycol) diacrylate (PEGDA) without using organic solvents, which could not only retain the bioactivity of ALP enzyme, but also protect the enzyme from digestive enzymes and gastric juice in stomach. As the alginate is a kind of pH responsive material, the alginate part of shell could be partially degraded and then the rest nondegradable PEGDA forms a porous structure with molecular sieving function in gut. Size of the pores could be precisely controlled through degrading a certain percentage of alginate, preventing outflow of ALP and inflow of digestive enzymes while allowing the permeation of LPS, which promised ALP's continuous function on detoxifying LPS in gut. We have also demonstrated that *in vivo*, this intelligent microcapsule could function as the scavenger to constantly englobe the LPS and detoxify it with ALP in the liquid cores, decrease intestinal permeability, regulate fat metabolism and reduce the inflammation. These indicated that the present intestinal scavenger microcapsules are valuable for internal secretion and biological detoxification.

2. Experimental section

2.1. Materials, cell lines, and animals

Photoinitiator 1173 (HMPP), PEGDA, alginate (low viscosity, Alfa Aesar), calcium chloride ($CaCl_2$), calcein-AM/PI (CA-PI), ALP, pepsin, pancreatin, potassium dihydrogen phosphate and phosphate buffer saline (PBS) were bought from Aladdin. LPS-fluorescein isothiocyanate (FITC) and CCK8 were bought from sigma. Hydrochloric acid (HCl) was bought from Nanjing Wanqing Chemical Glass ware and instrument Co., Ltd. Sodium hydroxide (NaOH) was bought from Nanjing Chemical Reagent Co., Ltd. Green fluorescent protein (GFP) was bought from Solarbio. Ethylenediaminetetraacetic acid disodium salt was bought from Sinopharm Chemical Reagent Co. Ltd. A high voltage power supply was gained from Gamma High Voltage Research. Caco-2 cells, Bovine Serum albumin-FITC, ALP kit (KGT043) and fibroblasts were gained from Keygene Company. Cells were cultured in Eagle's Minimum Essential Medium (EMEM, Gibco, USA) under the condition of 37 °C and 5% CO_2. The 8-12-week male mice were from Jinling Hospital. All animals were treated in strict accordance with the recommendations in the Guide for the Care and Use of Laboratory Animals of the National Institutes of Health, USA. All animals' experimental protocols and care were reviewed and approved by Animal Investigation Ethics Committee of the Jinling Hospital.

2.2. Microfluidic device design

The microfluidic device was fabricated of a glass slide and tapered capillaries. The outer capillary was tapered and sanded to reach a diameter of approximately 150 μm, and the inner capillary was pulled with a laboratory portable Bunsen burner (Honest Micro Torch) to form spindle tips. Then inner capillary was then coaxially inserted into the outer tapered capillary. Needles with crevices at the bottom were used at

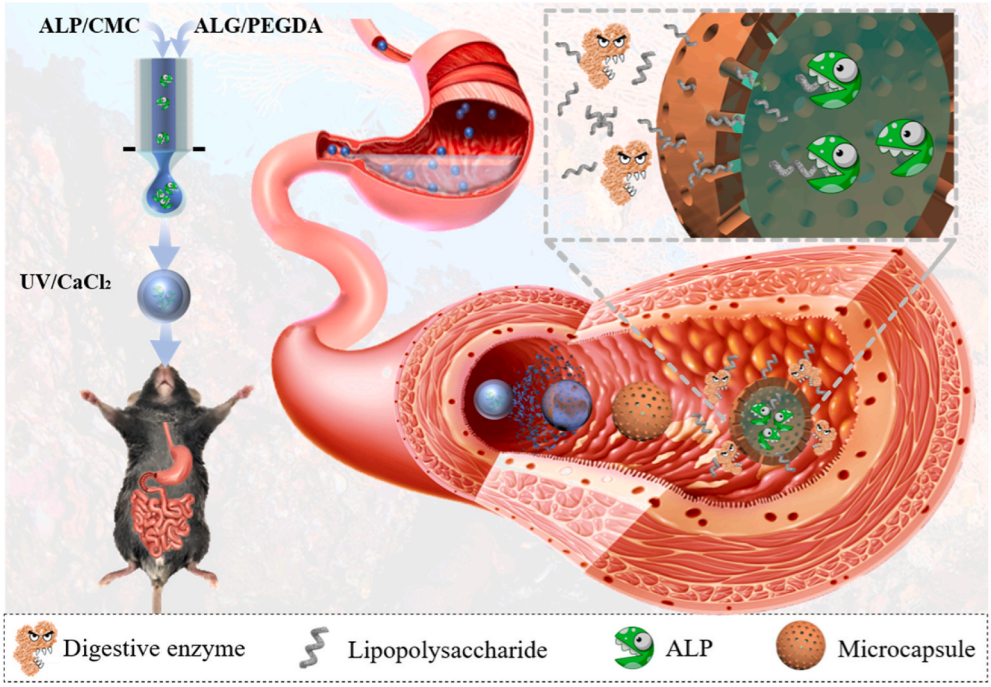

Fig. 1. Design and fabrication of the intestinal scavenger microcapsule. Schematic illustration of the fabrication and application of the microfluidic encapsulated porous A-microcapsules. The shell of the microcapsules could protect the contents in stomach and degrade in gut to form a precisely controlled porous structure which allowed the permeation of LPS and prevented the traverse of digestive enzymes.

the connection of the inner and outer capillary. Then, a transparent epoxy resin was used to seal the microfluidic device.

2.3. Fabrication of the microcapsules

Alginate was composed with PEGDA and HMPP to form the outer phase. ALP was composed with 1% CMC for the internal phase. High voltage was generated through a voltage power supply which provided electric field for the microfluidic electrospray. Owing to the low flow rate, low diameter and high viscosity in Reynolds numbers and hydrodynamic focusing effect, the compound jet formed laminar flows and stretched to Taylor cone entirely, and then broke into microdroplets at high voltage. The generated microdroplets were collected and gelled by a dish filled with 2% calcium chloride and UV for 1 h. For analysing the pore size, alginate and PEGDA were disposed at the ratio of 0%, 1%, 4%, 12% and 20% (w/w) to form gels and microcapsules with UV and calcium chloride. The size and morphology of microcapsules and gels were analysed under different voltage (U), collecting distance (d) and flow rate of inner (F_{inner}) and outer phase (F_{outer}). In this experiment, 12.5 kV voltage, 10 μL min^{-1} of inner flow rate and 50 μL min^{-1} of outer flow rate were applied to generate the microcapsule.

2.4. Characterization

ALP encapsulated microcapsules (A-microcapsule) were recorded by microscopy (OLYMPUS IX71) equipped with CCD cameras (DP30BW) for bright-field images. The microstructures of microcapsules were characterized by a scanning electron microscope (SEM, Navo Nano SEM450). Before SEM, samples were treated with 0.5% (w/v) EDTA for 2 h and then washed with ultrapure water for 3 times to remove the alginate and imitate the process in gut. Owing to the similar molecular weight, GFP was used to simulate the digestive enzymes. 100 μL of prepared 2 mg mL^{-1} LPS-FITC solution and 100 μL 50 μg mL^{-1} of GFP were separately added to the treated microcapsules and incubated for 1 h at room temperature. The microcapsules were then observed under a fluorescence microscope. The encapsulation efficiency was determined through BSA-FITC and a microplate reader. Briefly, BSA-FITC was composted with CMC to fabricate microcapsules. The concentration of BSA-FITC in the supernatant was assayed by microplate reader at 520 nm, and then subtracted by the total amount used. The encapsulation efficiency was defined as the ratio of the actual amount of encapsulated ALP over the used. Through regulating the initial concertation, the final amount of ALP could be controlled. The degradation of alginate was conducted in SIF. Briefly, alginate microspheres were fabricated through microfluidic electrospray. Later, these microspheres were immersed in SIF and observed through an optical microscopy at 0.5, 1, 1.5, 2 and 6 h.

2.5. Cytotoxicity tests of the microcapsules

1 mL EMDM was added to the resultant gels and incubated for 24 h. The fibroblasts were plated in 96-well culture dishes with 5000 cells per well (100 μL) and cocultured with pre-treated 1 mL EMDM for another 24 h. The cell viability was then measured through CA staining and recorded with a fluorescent microscope. CCK-8 assay was also conducted for quantitative analysis. Briefly, 10 μL CCK-8 PBS solution was added to each well and the plates were incubated for 2 h. The optical density (OD) of each well was measured using a microplate reader at 490 nm.

2.6. Analysing enzymatic activity of ALP after treated with digestive fluids

In vitro digestion models were conducted to evaluate the behaviour of ALP, alginate-ALP and A-microcapsule groups in digestive system. SGF (3.2 g mL^{-1} pepsin, 2 g L^{-1} NaCl and pH 1.5) and SIF (10 g mL^{-1} pancreatin, 6.8 g mL^{-1} potassium dihydrogen phosphate and pH 6.8) were prepared to imitate the digestion in alimentary tract according to previous research. The control groups were ALP group without SGF and SIF. Other groups were 0.7 U ALP (ALP group), 3% alginate microcapsule encapsulated 0.7 U ALP (ALG-ALP group) and 0.7 U PEGDA-alginate microcapsule encapsulated ALP (A-microcapsule group) treated with 20 μL SGF for 30 min. In SIF group, ALP, microcapsule and A-microcapsule were treated with SGF for 30 min and SIF for another 30 min. Before the activity test, A-microcapsules were treated with EDTA for to generate porous structures. To analyse ALP's activity, ALP and microcapsule were incubated with 100 μL disodium phenylphosphate (buffer A) and 100 μL 4-aminoantipyrine (buffer B). Then, the resultants were added with 300 μL potassium cyanide (buffer C) and heated in 37 °C water-bath and fetched out at 15 min, 30 min, 45 min, 12 h and 24 h. In this process, ALP degraded disodium phenyl phosphate into pbenol. Pbenol futher reacted with 4-aminoantipyrine, and the resultant could be catalyzed into red quinone derivatives by potassium cyanide. The result of enzyme activity is based on the indicator concentration of red quinone derivatives. The ALP kit (KGT043) is a common tool for detecting activity of ALP, and this experiment could only be done at neutral pH. To avoid the error in this process, we adjusted the pH in reactions after treated with SGF and SIF. Through the adjusting, the result would not be affected by pH.

2.7. Protection of microcapsules on cells

0.1 μg mL^{-1} LPS and 10^4 caco-2 cells were employed to build the MetS model. Normal cells without LPS was set as control. Three groups stimulated with LPS were set as experimental groups including LPS group, microcapsule group + LPS and A-microcapsule + LPS group. LPS, microcapsules and A-microcapsules were mixed for 12 h before cocultured with cells. Later, the supernatants were separated for cell experiment. After 24 h culture, the cells were stained with CA-PI to analyse the cell viability and protection of the microcapsules. A fluorescent microscope was used to record the images. Additionally, the inflammatory levels in different groups were further detected through ELISA according to manufacturer's instructions. The results were expressed with respect to the control.

2.8. Protection of microcapsules on mice

All animal tests were carried out according to the guidelines approved by the Animal Ethics Committee of Jinling Hospital affiliated to Medical School of Nanjing University. A mouse MetS model was employed to evaluate the effect of A-microcapsules on MetS preventing. During 8 weeks, a total of 15 healthy C57/BL mice were treated with a HFHS diet to induce MetS and 5 healthy C57/BL mice were fed with HFHS diet to set as control. This HFHS diet was fabricated as reported in the previous study [42]. Briefly, the HFHS diet included 20% casein high nitrogen, 0.18% L-cysteine, 26.9% sucrose FCC, 5% alphacel non-nutritive bulk, 6.7% mineral mix, 1.4% vitamin mix, 19.8% lard, 19.8% corn oil, 0.2% choline bitartrate and 0.03% tert-butylhydrytoluene. The normal diet included 19% crude protein, 6.2% fat, 44% carbohydrate, 3.5% crude fibre, 15% insoluble fibre and 5.3% ash. HFHS mice were divided into three groups, including microcapsule group, ALP group and A-microcapsule group, and treated with different interventions throughout 8 weeks. In microcapsule group, mice were treated with 500 mg empty microcapsule daily. In ALP group, mice were treated with 1000 units ALP in 100 μL PBS daily. In A-microcapsule group, mice were treated with 500 mg microcapsule encapsulated 1000 units ALP daily. This is the common dosage for mice experiment. At 8th week, all mice were sacrificed. Tissues were collected for further histology analysis. Blood was drawn in tubes for analysing inflammatory factors and blood biochemical factors. Inflammatory factors including IL-1 β, TNF-α and IL-6 were measured through ELISA according to the manufacturer's instructions. Briefly, the samples were prepared into supernatants, and then coated with monoclonal capture antibodies for 2 h. After washed with PBS, the cytokines were added with a horseradish

peroxidase-conjugated antibody. The resultant samples were further incubated and washed. Then, chromogenic substrate was added and the absorbance was measured at 450 nm. The concentrations of inflammatory factors were then determined through standard curves. Results were expressed with respect to control. Blood biochemical factors, including triglyceride, total cholesterol (TC), low-density lipoprotein (LDL), high-density lipoprotein (HDL), aspartate aminotransferase (AST), alanine aminotransferase (ALT) and glutamyl transpeptidase (GGT), were detected with a Tosoh-G8 analyser (Tosoh Bioscience, Japan) following the manufacturer's manual to analyse the lipid metabolism. We validated the disease model through the manifestations, including disruption of gut barrier proteins, increased intake of LPS in intestine, disordered fat metabolism and increased inflammation.

2.9. Histology analysis and immunofluorescence analysis

Before histology analysis, tissues were immersed in neutral formaldehyde for at least 24 h. Frozen liver tissues were stained with oil red and the pathological scores were graded based on the number and size of stained fat droplets. Other organs which included kidney, intestine, pulmonary, heart and spleen were dehydrated and embedded in paraffin for Hematoxylin-eosin (HE) staining. Afterwards, oil red o staining was conducted with a microtome to acquire a 5 μm serial sections. Sections for immunofluorescence staining were then incubated with ZO-1 or occludin-3 antibody at 4 °C overnights. Then, the sections were washed with PBS for three times and treated with secondary antibody (dissolved in 1% BSA) for 1 h at 25 °C. Images were recorded with an Olympus BX43 fluorescence microscope. To analyse the content of LPS in tissue, intestines were taken and measured with an LPS ELISA kit (Cusabio, CSB-E09945h) following the manufacturer's instructions. Briefly, tissues were pre-treated with 1 × PBS. Reagents were added to samples and incubated for 4.5 h at 37 °C, and the absorbance was read at 540 nm. Standard curve was conducted using known amounts of LPS.

2.10. Statistical analysis

All statistical analyses were conducted with SPSS 19.0. The data were presented as mean ± standard deviation. Statistical significance of the difference was determined by *t*-test. $P < 0.05$ was considered significant.

3. Results and discussion

3.1. Structural and morphological characterization

In a typical experiment, ALP encapsulated microcapsules (A-microcapsules) were fabricated with a coaxial capillary microfluidic chip (Fig. 2A). Owing to hydrodynamic focusing, the outer phase was sheathed around the inner CMC-ALP phase during the flowing. Then, the droplets were formed within the electric field and sprayed into UV area and the gelling bath which contained 2% $CaCl_2$. The fast gelation of alginate-Ca^{2+} and PEGDA could instantly solidify the shell structure of the microcapsule and encapsulate ALP in the core to form core-shell structure (Fig. 2B). Then, a porous shell could be fabricated through removing alginate with ethylenediaminetetraacetic acid disodium salt. The characteristics of the microcapsule were further observed in detail with SEM (Fig. 2C–F). Moreover, the encapsulation efficiency of microcapsules can reach 84%, and the dosages used later have already been calculated according to the encapsulation rate after conversion. By dynamically regulating voltage (U), outer phase flow velocity (F_{outer}), inner phase flow velocity (F_{inner}) and collecting distance (d), size of the microcapsules could be precisely controlled and good monodisperse could be achieved (Fig. S1 and Fig. S2). Theoretically, smaller size of the microcapsule contributes to the larger contact area and better effect. However, it is difficult to prepare smaller size of the microcapsule. In addition, smaller microcapsule could lead to undesirable wrapping effect and accelerated degradation. So, we chose microcapsules of a few hundred microns. Alginate could remain their structure in stomach and degrade in intestine owing to the different pH, which contributed to the protection of contents and formation of pores in shell (Figs. S3A and B). In low pH environment of gastric fluid, the microcapsules remained intact without a molecular sieving effect. When the microcapsules were in slightly alkaline environment of SGF, the alginate will degrade which lead to the generation of molecular sieving effect. After treated with low-pH SGF, the alginate still could degrade in SIF. So, it's conceivable that low pH values in stomach won't influence the molecular sieving effect [43]. Furthermore, the size of pore in the shell could be precisely controlled to act as molecular sieve by adjusting the ratio of alginate and PEGDA (Fig. S4). Thus, we could adjust the proportion of materials to advance a molecular sieving shell which could allow the absorption of LPS and inhibit the permeation of digestive enzymes.

3.2. Characterizing the ability of the molecular sieving

To identify the ability of molecular sieving, the resultant

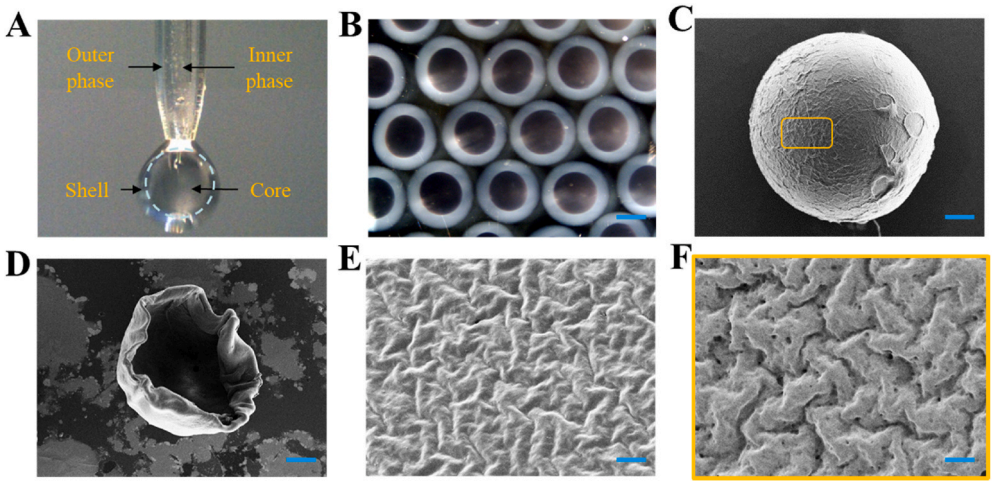

Fig. 2. Fabrication and characterization of the microcapsules. A) The real-time image of the microfluidic electrospray process. B) Bright field microscope images of the A-microcapsules. C–F) SEM images of the (C) A-microcapsule, (D) half dissected microcapsule, (E) the surface of shell, and (F) the outer surface of alginate-removed porous shell. Scale bars in (B) is 200 μm, in (C) is 50 μm, in (D) is 75 μm, in (E) and (F) is 2 μm.

microcapsules were characterized with fluorescence confocal. Microcapsules with different ratios of alginate/PEGDA were fabricated and cultured with LPS-FITC and GFP. In our opinion, pores could be fabricated and enlarged with the increase of alginate, which could regulate the permeation of molecules with different molecular weight (Fig. 3A). After 1 h coculture, 4%, 12% and 20% groups showed significantly increased intake of LPS-FITC which implied higher level permeation of small molecules. Due to the larger specific surface area provided by the porous structure, the scavenger microcapsules provide more sites for the adsorption of LPS-FITC, enabling LPS-FITC to be enriched inside the microspheres after a period (Fig. S5). GFP was used to imitate digestive enzyme owing to the similar molecular weight. In terms of GFP, it showed no significant permeation in 0%, 1%, 4% and 12% groups which indicated potential protection from digestive enzymes. However, the microcapsules in 20% groups showed more permeation of GFP which implied accelerated permeation of lager molecules with increased percentage of alginate (Fig. 3B-**D**). The quantified result also implied the successful formation of molecular sieving microcapsule which accelerate the permeation of small molecules (e.g. LPS) but retarded the traverse of larger molecules (e.g. digestive enzymes). The hydrogel microcapsules with molecule-selective permeability have been designed by microfluidic method, which could regulate the permeability of the shell according to the microenvironment. They have been applied in sensor platform, controlled release, enzyme capture and so on [44–46]. Thus, we believed our designed intestinal scavenger microcapsules have great potential in biomedical application and treating LPS associated diseases.

3.3. Analysing the biomedical potential of the microcapsules

To evaluate the biomedical application potential of the microcapsules, their biocompatibility was estimated. Microcapsules with different ingredient ratios were fabricated by changing the ratios of alginate and PEGDA. Then, 5000 cells were used to assess the cytotoxicity of the microcapsules through the extract solution, CAM staining and CCK-8 (Fig. 4). After 24 h culture, the results of cell fluorescence and CCK-8 indicated that the biocompatibility of pure PEGDA was poor when alginate was not incorporated. The biocompatibility of the microcapsules improved with the addition of sodium alginate. In different ratio groups, the 12% group showed best biocompatibility with most cell viability, which indicated its potential in biomedical application. At the same time, as the total amount of microcapsules decreases, the biosafety

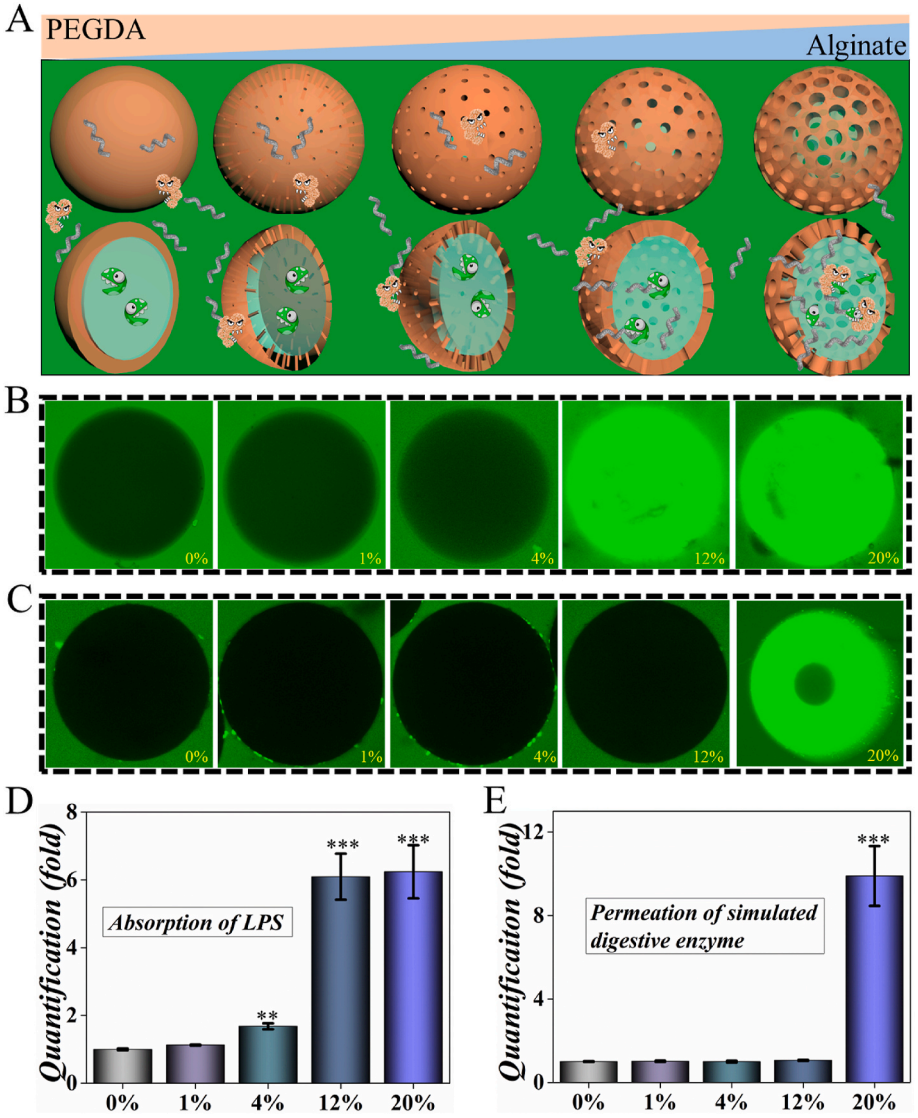

Fig. 3. Characterization of the molecular sieving system. A) Schematic illusion of the mechanism of molecular sieving system. B) Permeation of LPS in different microcapsules. C) Permeation of GFP in different microcapsules. D) The quantification of absorbed LPS in B). E) The quantification of permeated GFP in C). ** for $P < 0.01$ and *** for $P < 0.001$.

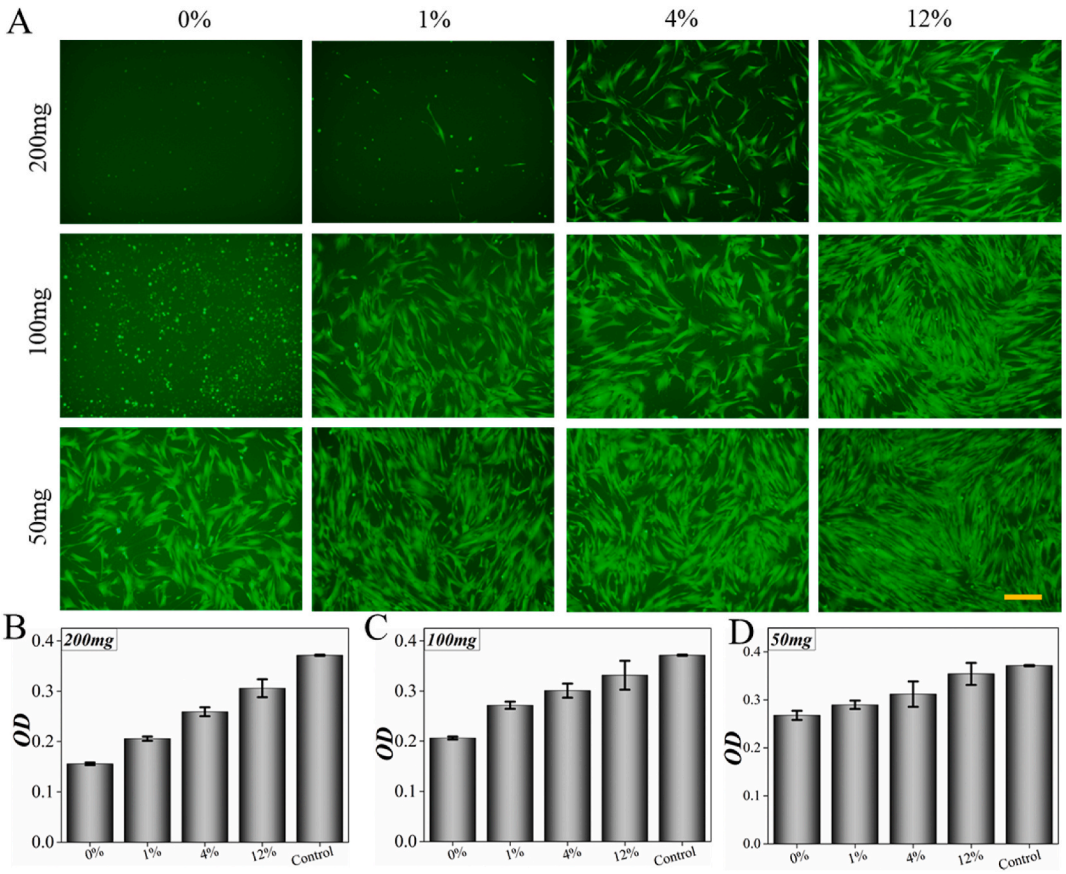

Fig. 4. Cytotoxicity experiment of shell material in different ratios and weights. A) Calcein AM staining of cells. B, C and D) OD value of cells coculturing with 200 mg shell material, 100 mg shell material and 50 mg shell material. Cell death decreased with the concentration of alginate and the weight of shell material after 24 h coculturing. Scale bar is 20 μm in (A).

of microcapsules was better when it was 100 mg or less. Through a series of optimizations, the appropriate ratio of shell for both biocompatible and molecular sieving system was set as 12%.

In digestive systems, the complex inner environment could impede the proteins' functions through digestive enzymes, gastric acid and so on, which limits the application of protein drugs. To investigate ALP's activity in digestive systems, A-microcapsules were incubated in simulated gastric fluid (SGF) and simulated intestinal fluid (SIF). Then, the resultants were collected and tested through ALP activity kits (Fig. 5). As it showed, the ALP group and alginate-ALP group showed very low level of enzymatic activity, while the A-microcapsule group showed significantly different after 15 min. Additionally, this group showed sustained effect during the following 30 min, which indicated the protecting effect of PEGDA-alginate shell against SGF and the function of detoxifying LPS through dephosphorylation and molecular sieving system (Fig. 5B). In all the groups, A-microcapsule group showed best activity and worked continuously during 24 h (Fig. 5C and Fig. S6). The presence of SIF influences reaction, so HCl was added to reduce this effect. As a result, the response speed of the microcapsules in the SIF-treated group was slower than the SGF-treated group. In this process, we were more concerned about the continuous working ability of the microcapsules in the intestine. The mechanics of microcapsules play an important role in their functions and should be reinforced. In the digestive process, the microcapsules must withstand the wear and tear associated to storage, transport and administration. Some studies use the ability of intestinal digestion to break the capsule to release drugs. In our experiments, the stable existence of the microcapsule in the digestive tract may contribute to better performance of the function of the contents [47]. The results demonstrated the effect of the porous-structure shell with molecular sieving function which could protect the contents from complex environment of digestive system and promise the function of the contents.

3.4. Validation on the effect of the microcapsules in vivo

In practical situations, the internalized LPS could be secreted into mesenteric lymph and systemic circulation, which induces chronic inflammation and damage of organs. Systemic and local inflammation lead to overexpression of inflammatory factors, which increases gut permeability and several symptoms of MetS. Hence, the capability of A-microcapsule to detoxify LPS and relieve the inflammation was also investigated. To further analyse the therapeutic effects of the A-microcapsule, cells were cultured with LPS and different interventions. The testing samples were divided into four groups, namely, control, LPS, empty microcapsule + LPS and A-microcapsules + LPS. It was found from the live-dead cell staining that the cells were alive in all groups while they are different in numbers. However, only the cells in A-microcapsule and control groups maintained their original appearance, which indicated therapeutic effect of the microcapsule (Fig. S7). Inflammation caused by LPS is the pathogeny of MetS and lead to disorders of organ function. Therefore, the anti-inflammatory capability of A-microcapsules was also measured in this study. LPS induced a serious inflammation in LPS and empty microcapsule + LPS group. However, in A-microcapsule group, the cells keep a relative high viability and low inflammatory levels. As the TNF-α and IL-6 decreased, these results indicated anti-inflammatory effect of the A-microcapsule in LPS induced diseases and we believe this effect contributed to relieving MetS.

To investigate the potential value of the A-microcapsule, a MetS murine model was constructed using a HFHS diet. The testing samples were divided into four groups, A-microcapsule, microcapsule, ALP and a

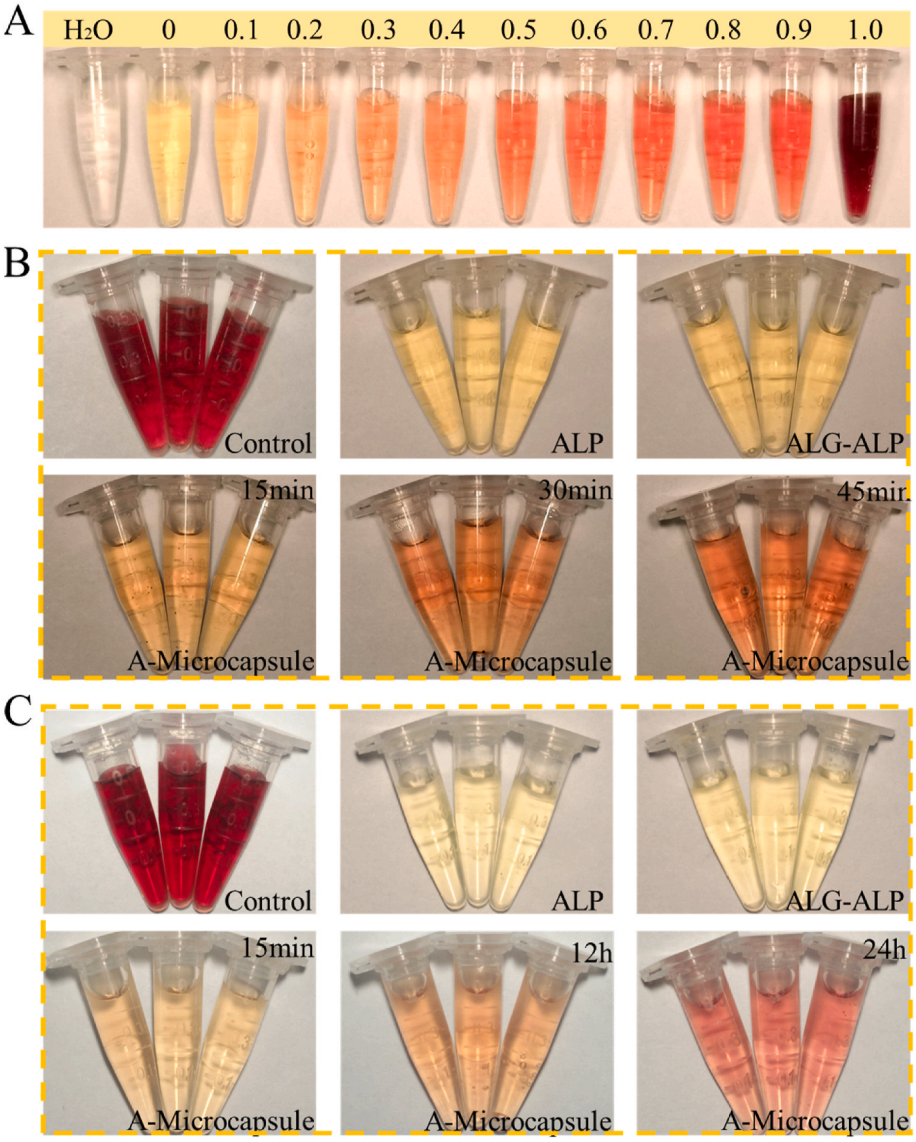

Fig. 5. Characterizing the enzymatic activity of ALP in digestive fluids. A) Standard curve of ALP's activity. B) ALP's activity of different groups in SGF with special focus on impact of digestive time changes on A-microcapsule. C) ALP's activity of different groups in SIF with special focus on impact of digestive time changes on A-microcapsule.

control group feeding HFHS without any intervention. From the microscale observation of immune staining, it was found that the barrier proteins density of claudin-1 and occludin in the intestine were clearly restored in the A-microcapsule group (Fig. 6A and B). Claudin-1 and occludin are important barrier proteins which regulate the permeation of the intestine; LPS could disrupt barrier functions and induce abnormal distribution of claudin-1 and occludin in diseases. Moreover, MetS related manifestations could drive intestinal barrier dysfunction and increase the permeation of LPS. In the pathogenesis of MetS, intestinal barrier function plays an important role in prevention and treatment [41]. Therefore, the correction of lost proteins is very important for treatment of MetS. The results implied that this intestinal scavenger microcapsule could effectively decrease intestinal hyperpermeability. As a result, the well protected intestinal barrier was likely to decrease the intake of LPS, as well as excessive fat, leading to the well-regulated metabolism (Figs. 6C and 7). The control group and microcapsule group showed greatest amount of fat deposit in liver oil red o staining which showed red staining. In contrast, the A-microcapsule group showed least amount of fat deposit in slides which implied better metabolism of lipid in liver (Fig. 6C).

MetS is a constellation of risk factors which often progress to severer metabolic diseases, including type 2 diabetes and liver diseases, leading to low degrade inflammation and disorders in metabolism. Through decreasing the intake of LPS, A-microcapsule could improve the metabolism system through regulating inflammation and fat metabolism (Fig. 7). In Fig. 7A, this A-microcapsule could reduce the level of LPS in intestine. Researches support the opinion that excessive enteric LPS leads to disorders in organs, and results in MetS finally [4–6]. Detoxifying LPS through dephosphorylation has great potential in treating MetS. In comparison with other groups, the bio-inspired intestinal scavenger could effectively prevent and treat the metabolic syndrome through detoxifying enteric LPS. Decreased fat deposit in A-microcapsule group led to lower level of AST, ALT and GGT in blood which implied a protective effect of the microcapsule on liver (Fig. 7B-D). Also, this group showed lowest level in the blood biochemical detection of triglyceride, TC, LDL, HDL and HDL/LDL, which implied decreased risk of cardiovascular disease (Fig. 7E-I). Herein, the microcapsule treated mice were protected from the metabolic disorder that occurs in response to HFHS induced MetS. IL-1β, TNF-α and IL-6 in serum were further tested to analyse the resulting systemic inflammation. In comparison

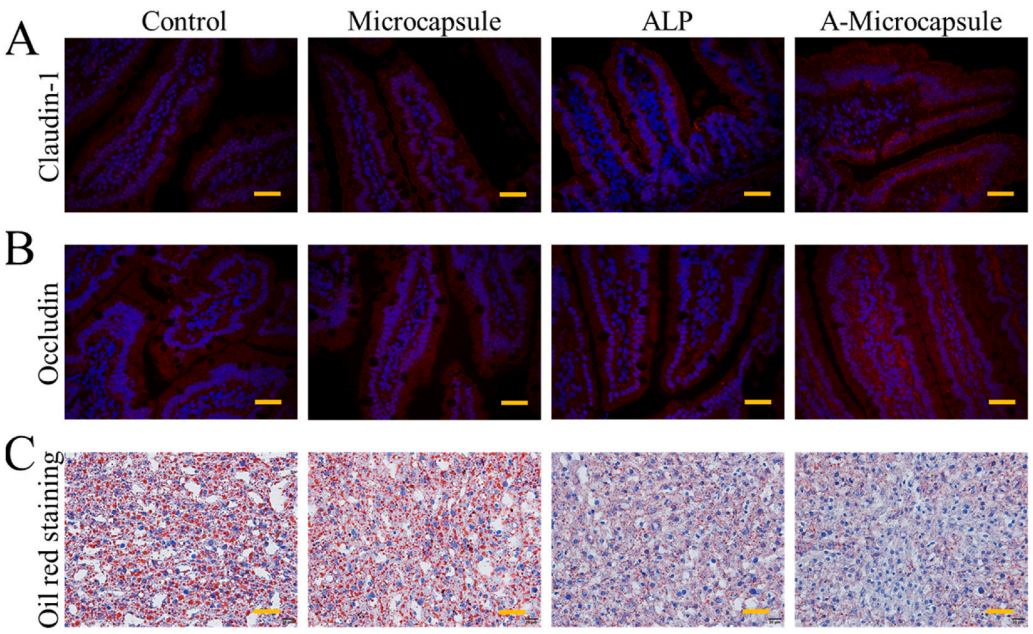

Fig. 6. Evaluation of therapeutic effect on preventing HFHS induced MetS. Intestinal immunofluorescence staining of gut barrier proteins, including claudin-1 (A) and occludin (B). C) Liver oil red o staining of mice with different interventions. Scale bars are 50 μm in (A) and (B) and 40 μm in (C). (For interpretation of the references to colour in this figure legend, the reader is referred to the Web version of this article.)

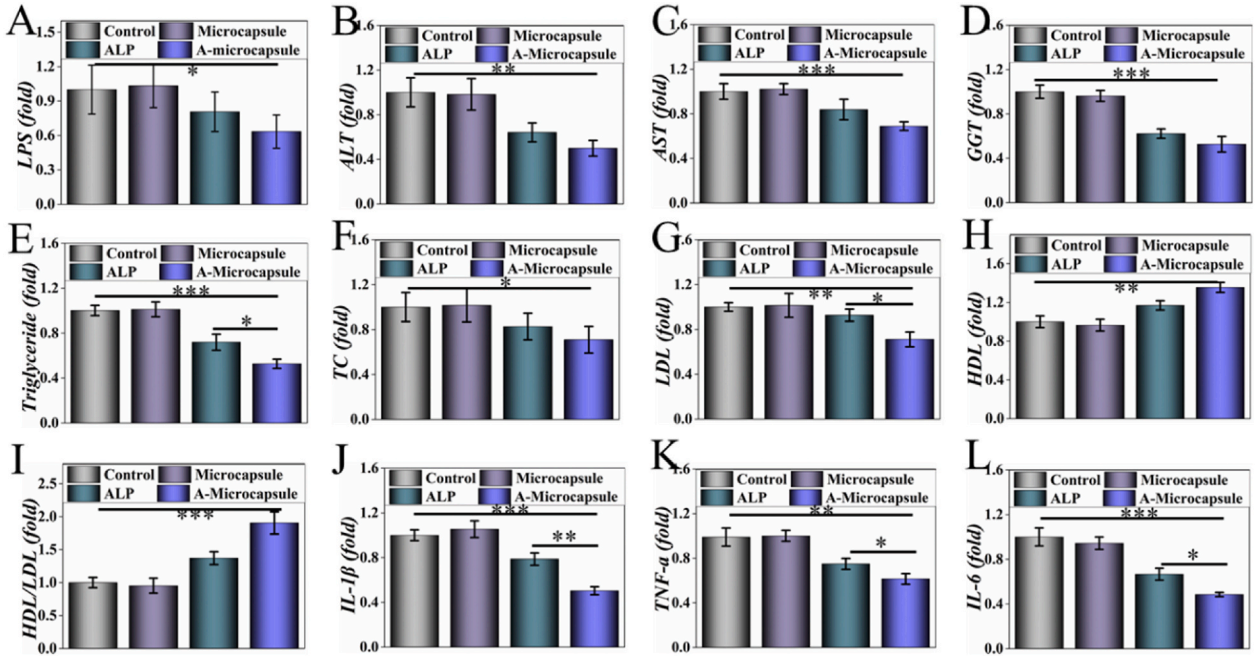

Fig. 7. A-microcapsules prevented HFHS diet induced MetS. A) The concentration of LPS in intestine. B–H) Blood biochemical factors of lipid metabolism in serum, including B) ALT, C) AST, D) GGT, E) triglgceride, F) TC, G) LDL, H) HDL and I) HDL/LDL. J, K, L) Inflammatory factors of J) IL-β, K) TNF-α and L) IL-6 in serum. * for $P < 0.05$, ** for $P < 0.01$ and *** for $P < 0.001$.

with other groups, the elevated level of inflammation could be reversed through the complement of A-microcapsule (Fig. 7J-L). *In vitro*, we used excessive the digestive juices and enzymes which are less in mice. So, there may be a small amount of ALP that can play a role before inactivation *in vivo*, but the efficiency was relatively low. These results demonstrated that the A-microcapsules were ideal materials for HFHS induced MetS through detoxifying LPS, protecting barrier function, regulating inflammation and restoring metabolism.

4. Conclusion

In conclusion, an intestinal scavenger from microfluidic encapsulated A-microcapsules for preventing LPS induced MetS has been built. These microcapsules were inspired by predatory ability of scavengers, which could englobe molecules of a specific size and purify the environment. Additionally, owing to the non-degradable feature of PEGDA, these resultant microcapsules could continuously work in gut to detoxify LPS through dephosphorylation. *In vitro*, we have demonstrated that through designing the shell, the microcapsule could protect ALP in SGF

and SIF. In addition, the A-microcapsule showed significantly improved function in mice. Through this work, we could protect ALP's activity in gastrointestinal which could highly improve its efficiency, and provide a way for utilizing bioactive substance in digestive tract. The practical value of the resulting A-microcapsules has been demonstrated through both of *in vitro* and *in vivo* experiments that LPS induced MetS could be relieved through restoring intestinal permeability, regulating fat metabolism and reducing inflammation. These features manifested that the A-microcapsules are efficient for preventing MetS, and thus we believe that these microcapsules have great potential in clinic.

Funding sources

This work was supported by the Strategic Priority Research Program of the Chinese Academy of Science (XDA16010303), National Key R&D Program of China (Nos. 2017YFA0103903, 2019YFA0111400), the National Natural Science Foundation of China (Nos.52073060, 82030029 and 81970882), Natural Science Foundation from Jiangsu Province (BE2018707 and BE2019711), , Shenzhen Fundamental Research Program (JCYJ20190814093401920), China Postdoctoral Science Foundation (2019M663108, 2019M653061) and Guangdong Basic Application Research Fund Project (2019A1515110925, 2019A1515111155).

CRediT authorship contribution statement

Cheng Zhao: Investigation, Formal analysis, Writing - original draft. **Guopu Chen:** Investigation, Formal analysis, Writing - review & editing, Validation. **Huan Wang:** Writing - review & editing. **Yuanjin Zhao:** Conceptualization, Methodology, Supervision. **Renjie Chai:** Conceptualization, Methodology, Supervision.

Declaration of interest

The authors declare that they have no known competing financial interests or personal relationships that could have appeared to influence the work reported in this paper.

Appendix A. Supplementary data

Supplementary data to this article can be found online at https://doi.org/10.1016/j.bioactmat.2020.11.017.

References

[1] A. Feraco, V. Marzolla, A. Scuteri, A. Armani, M.*. Caprio, Mineralocorticoid receptors in metabolic syndrome: from physiology to disease, Trends Endocrinol. Metabol.: TEM (Trends Endocrinol. Metab.) 31 (3) (2019) 205–217.
[2] C.R. Kahn, G. Wang, K.Y.*. Lee, Altered adipose tissue and adipocyte function in the pathogenesis of metabolic syndrome, J. Clin. Invest. 129 (2019) 3990–4000.
[3] J.P. Mann, D.B.*. Savage, What lipodystrophies teach us about the metabolic syndrome, J. Clin. Invest. 130 (2019) 4009–4021.
[4] A.L. Dinel, C. Andre, A. Aubert, G. Ferreira, S. Laye, N. Castanon, Lipopolysaccharide-induced brain activation of the indoleamine 2,3-dioxygenase and depressive-like behavior are impaired in a mouse model of metabolic syndrome, Psychoneuroendocrinology 40 (2014) 48–59.
[5] K. Kaliannan, S.R. Hamarneh, K.P. Economopoulos, S.N. Alam, O. Moaven, P. Patel, N.S. Malo, M. Ray, S.M. Abtahi, N. Muhammad, A. Raychowdhury, A. Teshager, M.M.R. Mohamed, A.K. Moss, R. Ahmed, S. Hakimian, S. Narisawa, J. L. Millan, E. Hohmann, H.S. Warren, A.K. Bhan, M.S. Malo, R.A. Hodin, Intestinal alkaline phosphatase prevents metabolic syndrome in mice, Proc. Natl. Acad. Sci. U.S.A. 110 (2013) 7003–7008.
[6] X. Liu, et al., Lipopolysaccharide binding protein, obesity status and incidence of metabolic syndrome: a prospective study among middle-aged and older Chinese, Diabetologia 57 (2014) 1834–1841.
[7] A. Iyer, J. Lim, H. Poudyal, R.C. Reid, J.Y. Suen, J. Webster, J.B. Prins, J. P. Whitehead, D.P. Fairlie, L. Brown, An inhibitor of phospholipase A2 group IIA modulates adipocyte signaling and protects against diet-induced metabolic syndrome in rats, Diabetes 61 (2012) 2320–2329.
[8] S. Pendyala, J.M. Walker, P.R.*. Holt, A high-fat diet is associated with endotoxemia that originates from the gut, Gastroenterology 142 (2012) 1100–1101.e1102.
[9] J.J. Wang, H. Tang, C.H. Zhang, Y.F. Zhao, M. Derrien, E. Rocher, J.E.T.V. Vlieg, K. Strissel, L.P. Zhao, M. Obin, J. Shen, Modulation of gut microbiota during probiotic-mediated attenuation of metabolic syndrome in high fat diet-fed mice, ISME J. 9 (2015) 1–15.
[10] R. Bellomo, J.A. Kellum, C.R. Gandhi, M.R. Pinsky, B. Ondulik, The effect of intensive plasma water exchange by hemofiltration on hemodynamics and soluble mediators in canine endotoxemia, Am. J. Respir. Crit. Care Med. 161 (2000) 1429–1436.
[11] F.H. Liao, T. Wu, C.N. Yao, S.C. Kuo, C.J. Su, U.S. Jeng, S.Y. Lin, Antibiotics evade endotoxin competition through A supramolecular trap for boosting anti-bacteremia activity, Angew. Chem. 132 (4) (2019).
[12] S.R. Hamarneh, M.M.R. Mohamed, K.P. Economopoulos, S.A. Morrison, T. Phupitakphol, T.J. Tantillo, S.S. Gul, M.H. Gharedaghi, Q.S. Tao, K. Kaliannan, S. Narisawa, J.L. Millan, G.M. van der Wilden, P.J. Fagenholz, M.S. Malo, R. A. Hodin, A novel approach to maintain gut mucosal integrity using an oral enzyme supplement, Ann. Surg. 260 (2014) 706–714.
[13] E. Peters, S. Geraci, S. Heemskerk, M.J. Wilmer, A. Bilos, B. Kraenzlin, N. Gretz, P. Pickkers, R. Masereeuw, Alkaline phosphatase protects against renal inflammation through dephosphorylation of lipopolysaccharide and adenosine triphosphate, Br. J. Pharmacol. 172 (2015) 4932–4945.
[14] C.T. Tian, J.J. Guo, G. Wang, B.J. Sun, K.X. Na, X.B. Zhang, Z.Y. Xu, M.S. Cheng, Z. G. He, J. Sun, Efficient intestinal digestion and on site tumor-bioactivation are the two important determinants for chylomicron-mediated lymph-targeting triglyceride-mimetic docetaxel oral prodrugs, Advanced science 6 (2019), 1901810.
[15] H. Wang, Z. Zhao, Y.X. Liu, C.M. Shao, F.K. Bian, Y.J. Zhao, Biomimetic enzymes cascade reaction system in microfluidic electrospray microcapsules, Sci. Adv. 4 (2018), eaat2816.
[16] C. Zhao, Y.R. Yu, X.W. Wu, J.A. Ren, Y.J. Zhao, Biomimetic intestinal barrier based on microfluidic encapsulated sucralfate microcapsules, Sci. Bull. 64 (2019) 1418–1425.
[17] Y.C. Chao, S.Y. Mak, S. Rahman, S.P. Zhu, H.C. Shum, Generation of high-order all-aqueous emulsion drops by osmosis-driven phase separation, Small 14 (2018), 1802107.
[18] S.Y. Cheng, Y. Jin, N.X. Wang, F. Cao, W. Zhang, W. Bai, W.F. Zheng, X.Y. Jiang, Self-adjusting, polymeric multilayered roll that can keep the shapes of the blood vessel scaffolds during biodegradation, Adv. Mater. 29 (2017), 1700171.
[19] H. Zhang, Y.X. Liu, J. Wang, C.M. Shao, Y.J. Zhao, Tofu-inspired microcarriers from droplet microfluidics for drug delivery, Sci. China Chem. 62 (2019) 87–94.
[20] Kim DJ, Park SG, Kim DH, Kim SH. SERS-Active-Charged microgels for size- and charge-selective molecular analysis of complex biological samples. Small, 14, 1802520.
[21] G.L. Ying, N. Jiang, S. Mahar, Y.X. Yin, R.R. Chai, X. Cao, J.Z. Yang, A.K. Miri, S. Hassan, Y.S. Zhang, Aqueous two-phase emulsion bioink-enabled 3D bioprinting of porous hydrogels, Adv. Mater. 30 (2018), 1805460.
[22] J. Wang, G.P. Chen, Z. Zhao, L.Y. Sun, M.H. Zou, J.A. Ren, Y.J. Zhao, Responsive graphene oxide microcarriers for controllable cell capture and release, Science China-Materials 61 (2018) 1314–1324.
[23] Y. Song, T.C.T. Michaels, Q.M. Ma, Z. Liu, H. Yuan, S. Takayama, T.P.J. Knowles, H.C. Shum, Budding-like division of all-aqueous emulsion droplets modulated by networks of protein nanofibrils, Nat. Commun. 9 (2018) 2110.
[24] W.S. Wang, J. Luo, S.T. Wang, Recent progress in isolation and detection of extracellular vesicles for cancer diagnostics, Advanced Healthcare Materials 7 (2018), 1800484.
[25] V. Balasubramanian, A. Domanskyi, J.M. Renko, M. Sarparanta, C.F. Wang, A. Correia, E. Makila, O.S. Alanen, J. Salonen, A.J. Airaksinen, R. Tuominen, J. Hirvonen, M. Airavaara, H.A. Santos, Engineered antibody-functionalized porous silicon nanoparticles for therapeutic targeting of pro-survival pathway in endogenous neuroblasts after stroke, Biomaterials 227 (2019), 119556.
[26] A.K. Miri, D. Nieto, L. Iglesias, H.G. Hosseinabadi, S. Maharjan, G.U. Ruiz-Esparza, P. Khoshakhlagh, A. Manbachi, M.R. Dokmeci, S.C. Chen, S.R. Shin, Y.S. Zhang, A. Khademhosseini, Microfluidics-enabled multimaterial maskless stereolithographic bioprinting, Adv. Mater. 20 (2018), 1800242.
[27] Q. Zhang, W. Wu, C.Y. Qian, W.S. Xiao, H.J. Zhu, J. Guo, Z.B. Meng, J.Y. Zhu, Z. L. Ge, W.G. Cui, Advanced biomaterials for repairing and reconstruction of mandibular defects, Materials Science & Engineering C-Materials for Biological Applications 103 (2019), 109858.
[28] J.R. Jiao, F.L. Zhang, T. Jiao, Z. Gu, S.T. Wang, Bioinspired superdurable pestle-loop mechanical interlocker with tunable peeling force, strong shear adhesion, and low noise, Advanced Science 5 (2018), 1700787.
[29] X.X. Zhang, Y.J. Zhao, Wearable droplet microfluidics, Sci. Bull. 64 (2019) 1472–1473.
[30] Lee TY, Ku M, Kim B, Lee S, Yang J, Kim SH. Microfluidic production of biodegradable microcapsules for sustained release of hydrophilic actives. Small, 13, UNSP 1700646.
[31] Y.X. Liu, Q. Huang, J. Wang, F.F. Fu, J.N. Ren, Y.J. Zhao, Microfluidic generation of egg-derived protein microcarriers for 3D cell culture and drug delivery, Sci. Bull. 62 (2017) 1283–1290.
[32] Z.L. Yang, Y. Yang, L. Zhang, K.Q. Xiong, X.Y. Li, F. Zhang, J. Wang, X. Zhao, N. Huang, Mussel-inspired catalytic selenocystamine-dopamine coatings for long-term generation of therapeutic gas on cardiovascular stents, Biomaterials 178 (2018) 1–10.
[33] C.M. Shao, Y.X. Liu, J.J. Chi, J. Wang, Z. Zhao, Y.J. Zhao, Photo-controllable inverse opal graphene hydrogel scaffolds with biomimetic enrichment capability for cell culture, Research 2019 (2019), 9783793.

[34] X.D. Ma, E. Ozliseli, Y.Z. Zhang, G.Q. Pan, D.Q. Wang, H.B. Zhang, Fabrication of redox-responsive doxorubicin and paclitaxel prodrug nanoparticles with microfluidics for selective cancer therapy, Biomaterials Science 7 (2019) 634–644.
[35] H.B. Zhang, X.M. Qu, H. Chen, H.X. Kong, R.H. Ding, D. Chen, X. Zhang, H. Pei, H. A. Santos, M.T. Hai, D.A. Weitz, Fabrication of calcium phosphate-based nanocomposites incorporating DNA origami, gold nanorods, and anticancer drugs for biomedical applications, Advanced Healthcare Materials 6 (2017), 1700664.
[36] Y. Liu, X. Jiang, Why microfluidics? Merits and trends in chemical synthesis, Lab Chip 17 (2017) 3960–3978.
[37] Y.N. Li, D. Yan, F.F. Fu, Y.X. Liu, B. Zhang, J. Wang, L.R. Shang, Z.Z. Gu, Y.J. Zhao, Composite core-shell microparticles from microfluidics for synergistic drug delivery, Science China-Materials 60 (2017) 543–553.
[38] G.P. Chen, Y.R. Yu, G.F. Wang, G.S. Gu, X.W. Wu, J.A. Ren, H.D. Zhang, Y.J. Zhao, Microfluidic electrospray vitamin metal-organic frameworks encapsulated microcapsules for wound healing, Research (2019), 6175398.
[39] L.L. Chaves, A. Silveri, A.C.C. Vieira, D. Ferreira, M.C. Cristiano, D. Paolino, L. Di Marzio, S.C. Lima, S. Reis, B. Sarmento, C. Celia, pH-responsive chitosan based hydrogels affect the release of dapsone: design, set-up, and physicochemical characterization, Int. J. Biol. Macromol. 133 (2019) 1268–1279.
[40] T. Miao, J. Wang, Y. Zeng, G. Liu, X. Chen, Polysaccharide-based controlled release systems for therapeutics delivery and tissue engineering: from bench to bedside, Advanced science 5 (2018), 1700513.
[41] C.A. Thaiss, M. Levy, I. Grosheva, D. Zheng, E. Soffer, E. Blacher, S. Braverman, A. C. Tengeler, O. Barak, M. Elazar, R. Ben-Zeev, D. Lehavi-Regev, M.N. Katz, M. Pevsner-Fischer, A. Gertler, Z. Halpern, A. Harmelin, S. Aamar, P. Serradas, A. Grosfeld, H. Shapiro, B. Geiger, E. Elinav, Hyperglycemia drives intestinal barrier dysfunction and risk for enteric infection, Science 359 (2018) 1376–1383.
[42] F.F. Anhê, T.V. Varin, M. Le Barz, et al., Arctic berry extracts target the gut-liver axis to alleviate metabolic endotoxaemia, insulin resistance and hepatic steatosis in diet-induced obese mice, Diabetologia 61 (4) (2018) 919–931.
[43] C. Zhao, Y. Zhu, B. Kong, Y. Huang, D. Yan, H. Tan, L. Shang, Dual-core prebiotic microcapsule encapsulating probiotics for metabolic syndrome, ACS Appl. Mater. Interfaces 12 (38) (2020) 42586–42594.
[44] B. Kim, H. Soo Lee, J. Kim, S.-H. Kim, Microfluidic fabrication of photo-responsive hydrogel capsules, Chem. Commun. 49 (2013).
[45] T.Y. Lee, S. Lee, Y.H. Kim, D.J. Kim, E. Amstad, C.S. Lee, S.H. Kim, Microfluidic fabrication of capsule sensor platform with double-shell structure, Adv. Funct. Mater. 29 (2019).
[46] J.G. Werner, S. Nawar, A.A. Solovev, D.A. Weitz, Hydrogel microcapsules with dynamic pH-responsive properties from methacrylic anhydride, Macromolecules 51 (2018) 5798–5805.
[47] M.P. Neubauer, M. Poehlmann, A. Fery, Microcapsule mechanics: from stability to function, Adv. Colloid Interface Sci. 207 (2014) 65–80.